Nanoscale Advances

Accepted Manuscript

This article can be cited before page numbers have been issued, to do this please use: B. Makiabadi, F. Naderi, M. Zakarianezhad and A. Raessi, *Nanoscale Adv.*, 2026, DOI: 10.1039/D5NA01168J.

ROYAL SOCIETY OF CHEMISTRY

rsc.li/nanoscale-advances

View Article Online
DOI: 10.1039/D5NA01168J

Investigation of cyclic peptides as drug delivery systems for the delivery of the anti-tuberculosis drug pyrazinamide

Batoul Makiabadi[a], Fereshteh Naderi[b*], Mohammad Zakarianezhad[c], Aria Raessi[d]

[a]Department of Chemical Engineering, Sirjan University of Technology, Sirjan, Iran

[b]Department of Chemistry, ShQ.C., Islamic Azad University, Shahr-e Qods, Iran

[c]Department of Chemistry, Payame Noor University (pnu), P.O.Box 19395-4697, Tehran, Iran

[d]Faculty of Medicine, University of Debrecen, 4032 Debrecen, Hungary

Abstract

One of the important goals of drug delivery in the treatment of diseases is to effectively deliver drugs to deep and inaccessible areas of tissues. In recent years, cyclic peptides (CPs) have been used as drug delivery systems due to their high affinity for their targets, stability against degradation, and low toxicity. In this study, the interaction of the anti-tuberculosis drug pyrazinamide (PY) with cyclic decapeptides of glycine, alanine, and serine and their binary alternating sequences was investigated at the M06-2X/6-31G(d,p) level of theory in the gas phase. Interaction energies, structural parameters, topological properties, as well as RDG, ELF, and IGM analyses were used to assess the strength of interactions in the complexes. The electronic properties of cyclic peptides were investigated and compared before and after the complexation process. Based on the findings of this study, cyclic peptides based on binary alternating sequences have a higher tendency to interact with the pyrazinamide molecule. Therefore, the use of a combination of amino acids in cyclic peptides allowed for the rational design of a new material with more favorable properties. These findings provide insights into the development of more effective drugs using cyclic peptides.

Keywords: Cyclic peptides; Anti-tuberculosis drug, Pyrazinamide, Interaction, Density functional theory, Ddrug delivery

* Corresponding Author: Fereshteh Naderi, Email:fnaderi@iau.ac.ir

View Article Online
DOI: 10.1039/D5NA01168J

Introduction

The delivery of therapeutic drugs to specific cells is a fundamental issue for the treatment of various human diseases, especially infectious, genetic, and cancer diseases. Developing drug delivery systems to penetrate and deliver drugs to target cells is a suitable solution for effective treatment of diseases [1-7]. Drug delivery systems are materials that prevent drug degradation, increase its effectiveness, reduce its side effects, and control its release at the desired site [8-11]. Recently, many studies have been conducted on the various properties of cyclic peptides and their role as drug carriers [12,13]. Cyclic peptides are polypeptide chains formed by the connection of the amino terminus and carboxyl group of the chain, forming cyclic structures. Compared to linear peptides, cyclic peptides show greater potential for biological activities, due to stable shape and state resulting from their cyclic structure [14-17]. Cyclic peptides have a high affinity for binding to target tissue due to their large surface area. Due to their cyclic nature, these structures have less flexibility and more rigidity, and are therefore more stable [18-21]. By changing the number and type of amino acids in cyclic peptides, the properties of cyclic peptides can be modified as drug delivery systems [22-24]. Wang and colleagues investigated the physicochemical properties of various types of cyclic peptides as drug delivery systems [25]. Fakhari and co-workers reported that the cyclic peptides cyclo[$(Ser\text{-}Ser)_4$], cyclo[$(Gly\text{-}Gly)_4$], and cyclo[$(Ala\text{-}Ala)_4$] could be effective carriers for the drug metformin [26]. A theoretical study was conducted on the properties of the cyclooctaglycine as a carrier for the anti-cancer drug penicillamine [27].

Given the global importance of infectious diseases and the need for effective drug delivery, tuberculosis one of the deadliest infectious diseases worldwide [28,29]. The most common types of drugs used to treat tuberculosis are rifampin, pyrazinamide, and streptomycin. Among the drugs used, pyrazinamide (PY) has shown good performance in treating patients with tuberculosis, by reducing side effects (fever, anorexia, liver enlargement, jaundice, and liver failure) and treatment duration [30,31]. However, current treatment methods have limited effectiveness due to poor patient compliance with the drug regimen or due to the presence of drug-resistant tuberculosis. In recent years, studies have been conducted on the delivery of anti-tuberculosis drugs. [32-36]. Research shows that anti-tuberculosis drugs can be encapsulated in liposomes, microparticles, or nanoparticles for controlled entry and release into lung cells [37-

View Article Online
DOI: 10.1039/D5NA01168J

39]. The use of these therapeutic methods in infected animals shows a significant increase in treatment improvement and reduction in complications and tissue damage [40,41].In addition to lipid-based and polymeric systems, various nanostructures such as carbon nanotubes (CNTs), fullerenes, boron-nitride nanotubes (BNNTs), and cyclic peptides have been widely investigated as carriers for pyrazinamide [31,42-44]. Although CNTs and BNNTs have high mechanical strength and thermal stability, cyclic peptides have often attracted more attention for drug delivery applications due to their biodegradability, low toxicity, and ease of chemical modification through sequence engineering. Cyclic peptides have the ability to precisely tune the chemistry of the internal cavity by changing the amino acid sequence. This ability to tune the sequence is the main motivation for the present study.

Therefore, in this project, the interaction of the anti-tuberculosis drug PY with cyclic decapeptides of glycine, alanine, and serine and their binary alternating sequences was studied. Studying how drugs bind to cyclic peptides could lead to the design of molecules with higher affinity and fewer side effects. In this study, the complexes resulting from the interaction of the PY with a variety of cyclic peptides were investigated. In this regard, structural parameters, interaction energies, atomic charge distribution, energy gap, electrostatic potential levels, charge transfer, and interactions strength were analyzed. This study attempts to answer the fundamental question, "What effect does changing the amino acid sequence in cyclic peptides have on the interaction with the drug pyrazinamide?" Therefore, in this work, we answer this question by systematically changing the CP sequence. By changing the amino acid sequence in cyclic peptides, an understanding of the structure-function relationship can be achieved, which allows for the rational design of drug carriers based on sequence chemistry. These insights are inaccessible when only a single sequence is studied. It is hoped that this study will provide a better understanding of how drugs bind and the role of the cyclic peptide structure, which could lead to the design of drugs with better absorption in the body.

Computational Methods

Density functional theory (DFT) was used to investigate the interaction of the drug PY with a number of cyclic decapeptides made of alanine, glycine, and serine amino acids. All structures were optimized at the M06-2X/6-31G(d,p) level of theory using the Gaussian 09 software package [45]. The counterpoise procedure (CP) [46] was used to correct for basis set

View Article Online
DOI: 10.1039/D5NA01168J

superposition error (BSSE) in the calculation of different binding energies. The interaction energy (ΔE_{ads}) is calculated as:

$$\Delta E_{int} = E_{(Comp)} - (E_{(PY)} + E_{(CP)}) \quad (1)$$

where, $E_{(Comp)}$ is the total energy of the complex of the drug interacting with the cyclic peptide, $E_{(PY)}$ is the total energy of a drug molecule, and $E_{(CP)}$ is the total energy of cyclic peptide. For all complexes, the molecular descriptors such as the HOMO–LUMO energy gap (E_{gap}), hardness (η), softness (S), electrophilicity index (ω)) and the maximum amount of electronic charge (ΔN_{max}) as:

$$E_{gap} = E_{LUMO} - E_{HOMO} \quad (2)$$

$$\eta = (Eg)/2) \quad (3)$$

$$S = 1/(2\eta) \quad (4)$$

$$\omega = (\mu^2/2\eta) \quad (5)$$

$$\Delta N_{max} = - \mu/\eta \quad (6)$$

When two systems A and B approach each other, the amount of charge transfer between them can be written in terms of electrophilicity. Electrophilicity-based charge transfer (ECT) is obtained by:

$$ECT = (\Delta N_{max})_A - (\Delta N_{max})_B \quad (7)$$

that if ECT > 0 then A is an electron acceptor, while if ECT < 0 it is an electron donor [47].

The solvent effect was examined using the M06-2X/6-31G(d,p) level of theory by applying the polarizable continuum model (PCM) [48]. Multiwfn program was used to plot the electron density of states (DOS), the electron localization function (ELF) [49], and independent gradient model (IGM). The reduced density gradient (RDG) plots were rendered by the VMD program [50] based on the outputs of Multiwfn. The NBO and AIM analysis was carried out at the M06-2X/6-31G(d,p) level of theory [51,52].

View Article Online
DOI: 10.1039/D5NA01168J

Results and discussion

Energies and Geometries

DFT calculations were performed to evaluate the interaction of the PY drug with a number of the cyclic peptides. The difference between these cyclic peptides is in the type and alternating sequence of amino acids used in them. In this regard, three types of amino acids were selected, such as alanine, glycine, and serine molecules (Scheme 1).

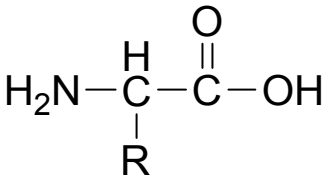

Amino acide	R
Glycine (G)	H
Alanine (A)	CH_3
Serine (S)	CH_2OH

Scheme 1. The linear structure of the amino acids Glycine, Alanine, and Serine

In the first stage, cyclic peptides composed of one type of amino acid were designed. Using 10 molecules of each, cyclic structures $CP_{X\text{-}X}$ (X=S, G, and A) were constructed and named as $CP_{G\text{-}G}$, $CP_{A\text{-}A}$, and $CP_{S\text{-}S}$ (See Figure 1).

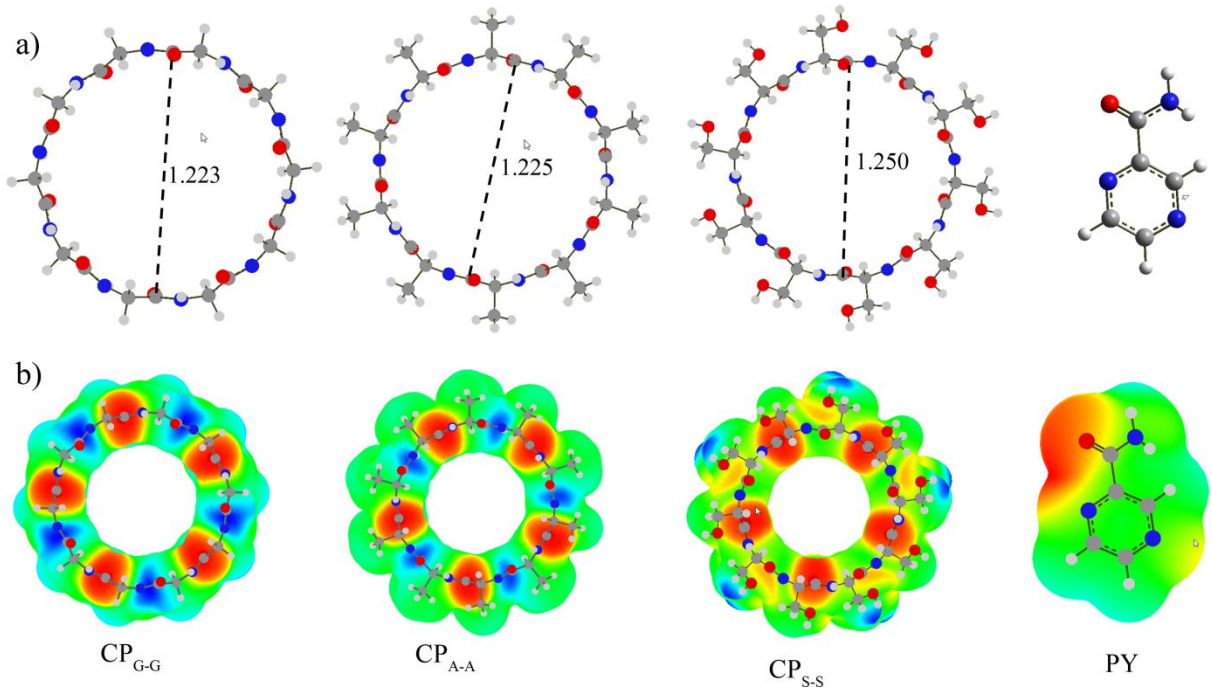

View Article Online
DOI: 10.1039/D5NA01168J

Figure 1. a) The optimized structures, b) the molecular electrostatic potential surface maps for $CP_{G\text{-}G}$, $CP_{A\text{-}A}$, $CP_{S\text{-}S}$, and PY structures.

As seen in the optimized structures, the oxygen atoms of the ketone groups are located alternately up and down of the cyclic peptides. It is observed that the length of C=O, C-C, and C-N bonds increases with the change of R group from hydrogen to methanol. Therefore, it is observed that the length of C-N bonds depends on the R group. The ring diameter from the carbon of the carbonyl group to the carbon of the opposite carbonyl group in $CP_{G\text{-}G}$, $CP_{A\text{-}A}$, and $CP_{S\text{-}S}$ is 1.223, 1.225, 1.250 Å, respectively. MESP (The molecular electrostatic potential surface) maps were drawn for the drug and different cyclic peptides (Figure 1). These maps were used to identify suitable sites on the drug and cyclic peptide for interaction with each other. In these color maps, red, blue, and green colors correspond to areas with negative, positive, and zero electrostatic potential, respectively. As can be seen, the oxygen atoms of the drug and the cyclic peptides have negative ESP, while the hydrogen atoms connected to N atoms have positive MESP. Therefore, the negative charges were placed on O atoms, while the positive charges were placed on H atoms. In $CP_{S\text{-}S}$, $CP_{G\text{-}G}$, $CP_{A\text{-}A}$, and PY structures, the average electrostatic potential values (ESP) on the local surface of the O atom of the C=O group is observed with values of -19.8, -22.5, -31.5, and -32.7 kcal/mol, respectively. Therefore, these sites are susceptible to electrophilic attack. In contrast, the average of ESP on the local surface of hydrogen atoms is positive, and thus nucleophilic reagents tend to be attracted to these sites.

In the first step, the DFT calculations were performed to evaluate the interaction of the PY drug with $CP_{S\text{-}S}$, $CP_{G\text{-}G}$, and $CP_{A\text{-}A}$ cyclic peptides. The most stable structures, named $CP_{S\text{-}S}$/PY, $CP_{G\text{-}G}$/PY, and $CP_{A\text{-}A}$/PY complexes (See Figure 2). Two types of hydrogen bonds, O…H and N…H, are observed in these complexes.

View Article Online
DOI: 10.1039/D5NA01168J

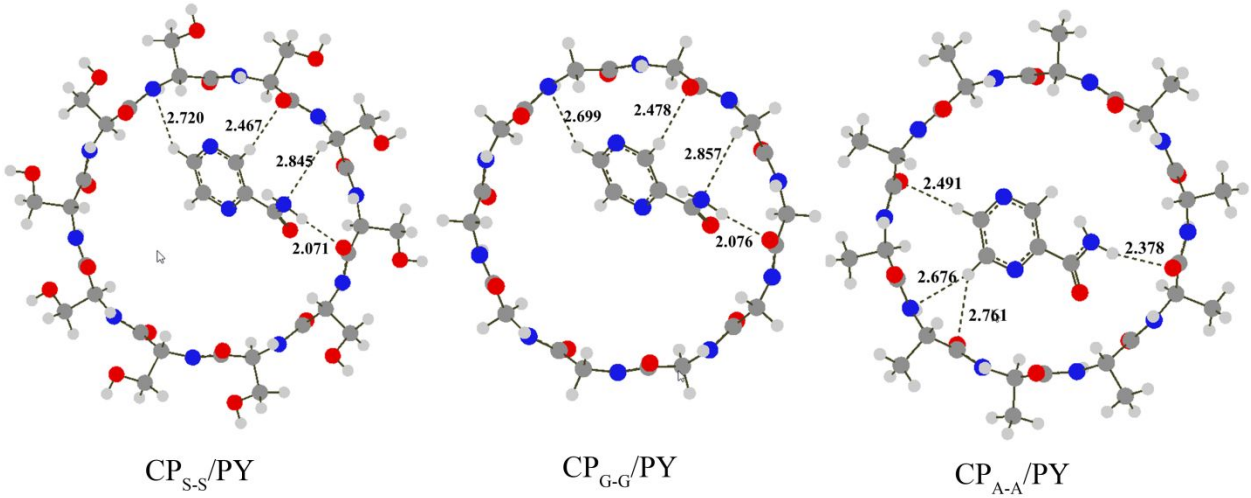

Figure 2. The optimized structures for CP$_{X-X}$/PY complexes at M06-2X/6–31G(d,p) level of theory

Analysis of structural parameters in CP$_{S-S}$/PY and CP$_{G-G}$/PY complexes shows that in the interaction between the drug and the cyclic peptide, two O...H hydrogen bonds and two N...H hydrogen bonds are formed, while in the CP$_{A-A}$/PY complex, three O...H hydrogen bonds and one H...N hydrogen bond are observed. Hydrogen bonds play important roles in biological systems [53-55]. In the CP$_{X-X}$/PY complexes, the lengths of the O···H hydrogen bonds are shorter than the N…H hydrogen bonds. These data suggest that O…H hydrogen bonding interactions are stronger than N…H interactions. On the other hand, the O...H hydrogen bond distances in the CP$_{S-S}$/PY complex are shorter than those in the CP$_{G-G}$/PY and CP$_{A-A}$/PY complexes. It is predicted that the O...H hydrogen bonding interactions in the CP$_{S-S}$/PY complex are stronger than the CP$_{G-G}$/PY and CP$_{A-A}$/PY complexes.

Studies show that the orientation of functional groups affects the spatial structure, stability, biological activity, and physicochemical properties of cyclic peptides. Therefore, the sequence of amino acids in the structure of cyclic peptides is of particular importance. To investigate this issue, the cyclic structures CP$_{X-Y}$/PY(X=S, G, A and Y=S, G, A, X≠Y) were considered. In these structures, the amino acids serine, glycine, and alanine were alternately substituted in CP$_{X-X}$/PY complexes. The resulting structures were named CP$_{S-A}$/PY, CP$_{S-G}$/PY, CP$_{G-S}$/PY, CP$_{G-A}$/PY, CP$_{A-G}$/PY, CP$_{A-S}$/PY, CP$_{S-S}$/PY, CP$_{G-G}$/PY, and CP$_{A-A}$/PY complexes. The CP$_{X-Y}$/PY optimized complexes at the M06-2X/6-31G(d,p) level of theory are shown in Figure 3.

View Article Online
DOI: 10.1039/D5NA01168J

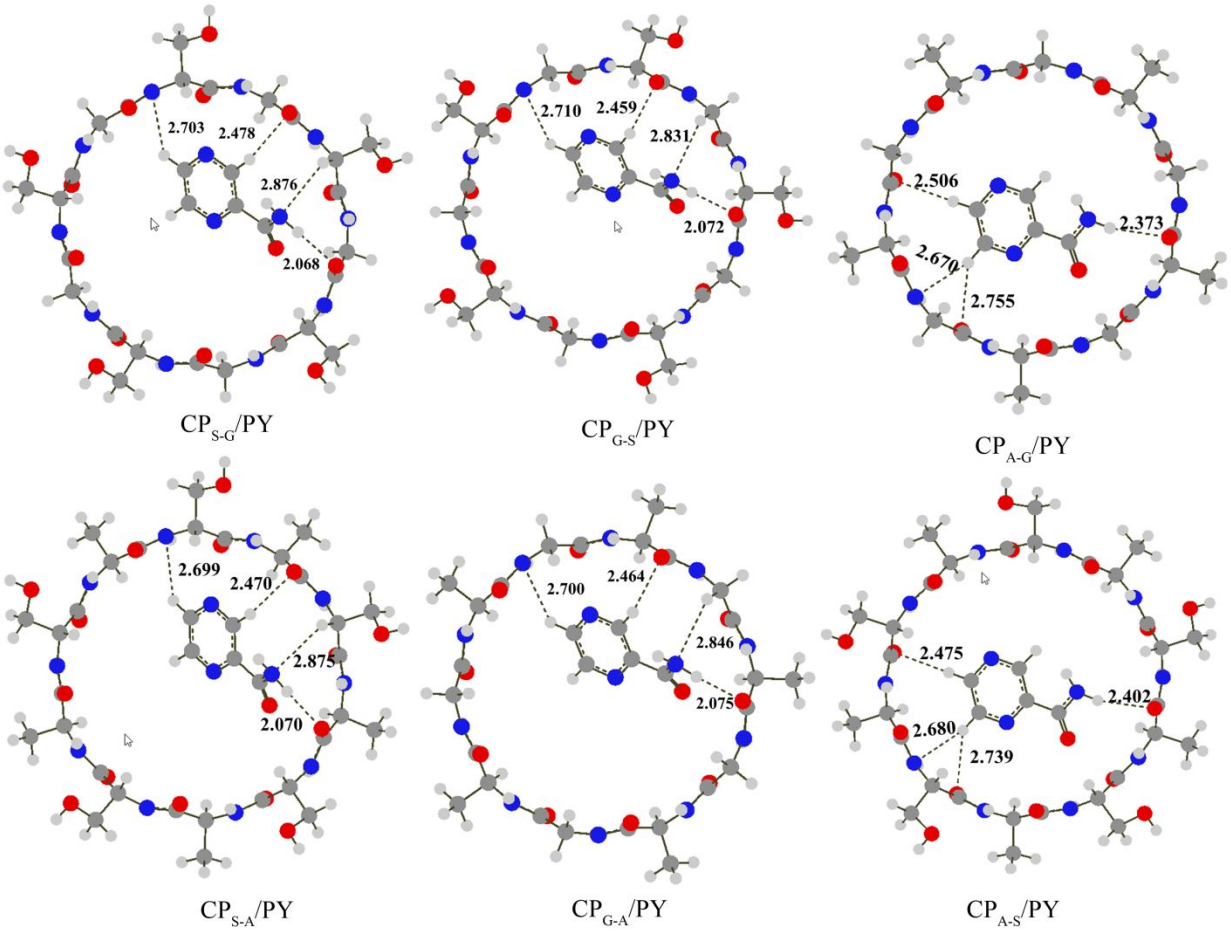

Figure 3. The optimized structures for CP_{X-Y}/PY complexes at M06-2X/6–31G(d,p) level of theory

The number and type of hydrogen bonds observed in CP_{X-Y}/PY complexes are similar to those in CP_{X-X}/PY complexes. Also, in these complexes, the drug is closer to the cyclic peptide from the NH_2CO side. The shortest hydrogen bond distance is 2.068 Å in CP_{S-G}/PY, 2.070 Å in CP_{S-A}/PY, 2.072 Å in CP_{G-S}/PY, 2.075 Å in CP_{G-A}/PY, 2.373 Å in CP_{A-S}/PY and 2.402 Å in CP_{A-G}/PY. This distance appears (O…H hydrogen bond) to be shorter and stronger in CP_{X-Y}/PY complexes than in CP_{X-X}/PY complexes.

The interaction energies (ΔE_{int}) for CP_{X-X}/PY and CP_{X-Y}/PY complexes at two theoretical levels have been summarized in Table 1. Based on the Table 1, the relative stability of complexes decreases in the order CP_{S-G}/PY> CP_{S-A}/PY> CP_{G-S}/PY> CP_{G-A}/PY> CP_{A-G}/PY> CP_{A-S}/PY> CP_{S-S}/PY> CP_{G-G}/PY> CP_{A-A}/PY. The results show that the ΔE_{int} values for CP_{X-Y}/PY complexes are more than those for CP_{X-X}/PY complexes. Therefore, structures with more

View Article Online
DOI: 10.1039/D5NA01168J

negative interaction energies are more stable. Also, the type and sequence of amino acids in cyclic peptides affect their stability. According to the results obtained, it can be concluded that CP_{X-Y}/PY structures are more stable than CP_{X-X}/PY complexes. It can be concluded that CP_{X-Y}/PY complexes have a higher affinity for drug interaction than CP_{X-X}/PY complexes. The interaction energy results show that the stability order of the complexes remained unchanged by changing the basis set.

Table 1 The interaction energies (ΔE_{int}/kJmol^{-1}), the recovery time (τ), charge transfer, and the hydrogen bonds energy (E_{HB}, kcal/mol) for all complexes

Structure	ΔE_{int}	ΔE_{int}^{bsse}	τ(s)	CT(e)	E_{HB}
CP_{S-S}/PY	-88.74 [a] (-78.50) [b]	-63.04	$3.1*10^{3}$	-0.00004	0.185
CP_{G-G}/PY	-43.64(-20.56)	-28.22	$4.1*10^{-5}$	-0.00180	0.180
CP_{A-A}/PY	-18.52(-16.03)	-5.53	$1.7*10^{-9}$	-0.00840	0.104
CP_{S-G}/PY	-100.80 (-95.58)	-69.88	$3.8*10^{5}$	-0.00186	0.195
CP_{S-A}/PY	-90.29 (-89.41)	-59.63	$5.2*10^{3}$	-0.00008	0.189
CP_{G-S}/PY	-88.84 (-86.32)	-57.96	$3.5*10^{3}$	-0.00192	0.187
CP_{G-A}/PY	-88.31 (-79.05)	-57.45	$2.4*10^{3}$	-0.00188	0.184
CP_{A-G}/PY	-68.65 (-62.10)	-42.59	$0.1*10^{1}$	-0.0094	0.102
CP_{A-S}/PY	-67.63 (-60.75)	-41.70	$6.7*10^{2}$	-0.00879	0.072

a: Interaction energies at the M06-2X/6-31G(d,p) level of theory
b: Interaction energies at the M06-2X/6-311++G(d,p) level of theory

The Espinosa-Molins-Lecomte (EML) equation (E_{HB}=0.5×V(r)) is a formula used to estimate the energy of hydrogen bonds, where V(r) is the value of local potential energy at the bond critical point [56]. The absolute value of E_{HB} ($|E_{HB}|$) for the shortest hydrogen bond (O…H) is reported in Table 1. The E_{HB}($|E_{HB}|$) value depends on the length of the hydrogen bond, so the shorter bonds have more ($|E_{HB}|$) and vice versa. In CP_{X-Y}/PY complexes, the absolute value of E_{HB}($|E_{HB}|$) related to O…H hydrogen bond is greater than that of CP_{X-X}/PY complexes. This result is consistent with the shorter and stronger O…H interaction in CP_{X-Y}/PY complexes than in CP_{X-X}/PY complexes. The recovery time (τ) is a critical parameter for gas sensors and drug delivery systems [57]. The term "recovery time" refers to the time required for a drug molecule to dissociate from the substrate surface. The recovery time can be calculated using conventional transition state theory ($\tau = \nu_0^{-1} \times \exp^{-\Delta E_{int}/kT}$) [58]. Where ΔE_{int} is the interaction energy, T is the ambient temperature (298.15K), k is the Boltzmann constant, and ν_0 is assumed to be 10^{12} Hz. We used this formula as a measure to compare the strength of drug binding to the cyclic peptides. The calculated time is used solely to compare the relative strength of interactions in

View Article Online
DOI: 10.1039/D5NA01168J

different structures. High interaction energy indicates a strong interaction between the drug and the cyclic peptide and can lead to a longer recovery time. The results of Table 1 show that the recovery time for CP_{X-Y}/PY complexes is longer than that of CP_{X-X}/PY complexes, which is in agreement with the greater interaction energy of CP_{X-Y}/PY complexes than CP_{X-X}/PY ones. The CP_{X-Y}/PY complexes are more stable than CP_{X-X}/PY complexes and hold the drug for a longer period of time, whereas CP_{X-X}/PY complexes release the drug rapidly, making them suitable for use in sensors. Therefore, the CP_{X-Y}/PY complexes are better for drug delivery due to their longer τ.

The electronic properties of structures

The positions of the highest occupied (HOMO) and lowest unoccupied (LUMO) molecular orbitals determine the electronic properties and reactivity of the structures. HOMO and LUMO orbitals referred to as electron donating and electron accepting orbitals, respectively. The charge distribution of HOMO and LUMO orbitals for monomers and complexes is given in Figures 4 and 5.

View Article Online
DOI: 10.1039/D5NA01168J

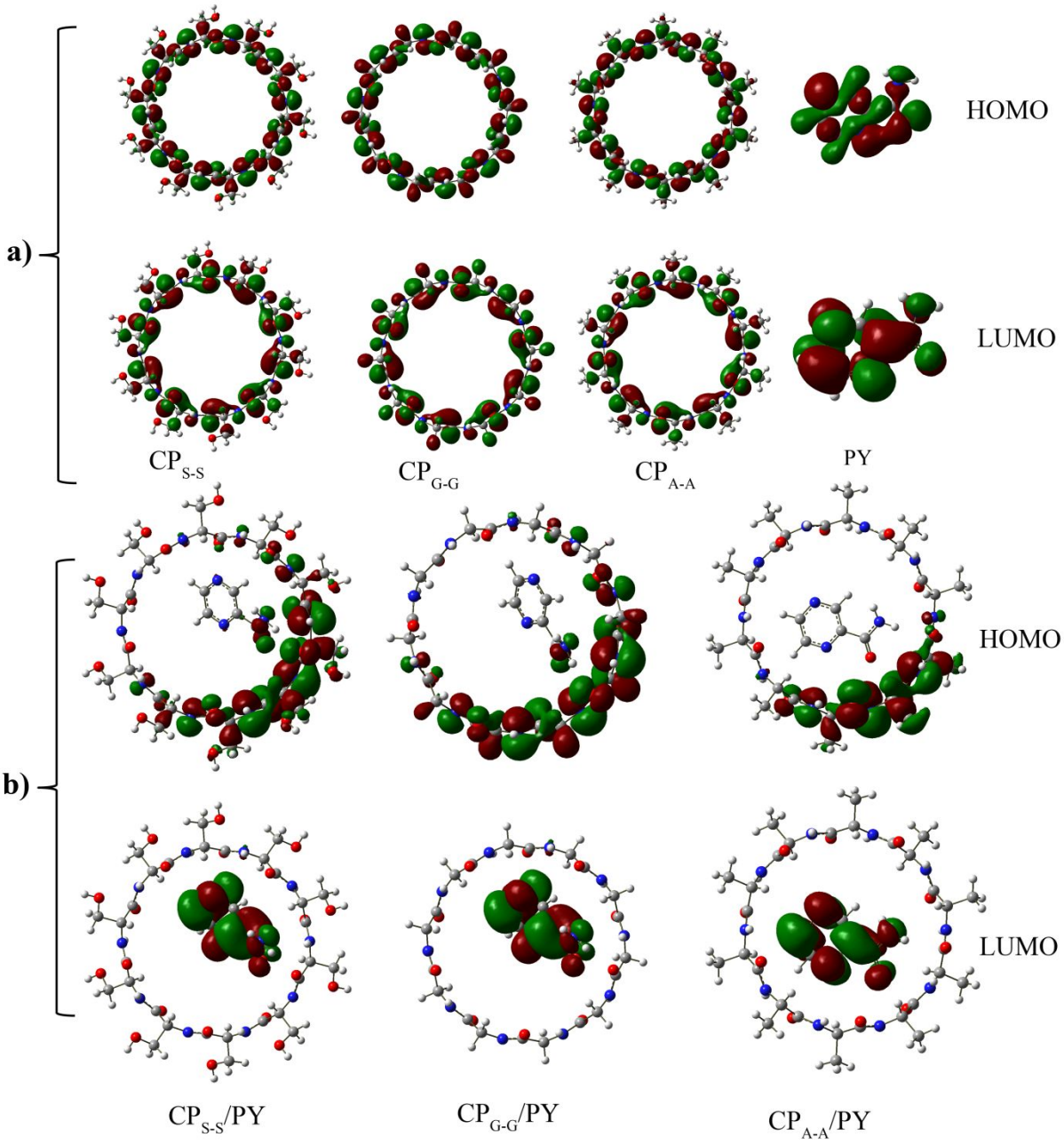

Figure 4. Charge distribution of HOMO and LUMO orbitals for a) monomers and b) the CP_{X-X}/PY complexes

View Article Online
DOI: 10.1039/D5NA01168J

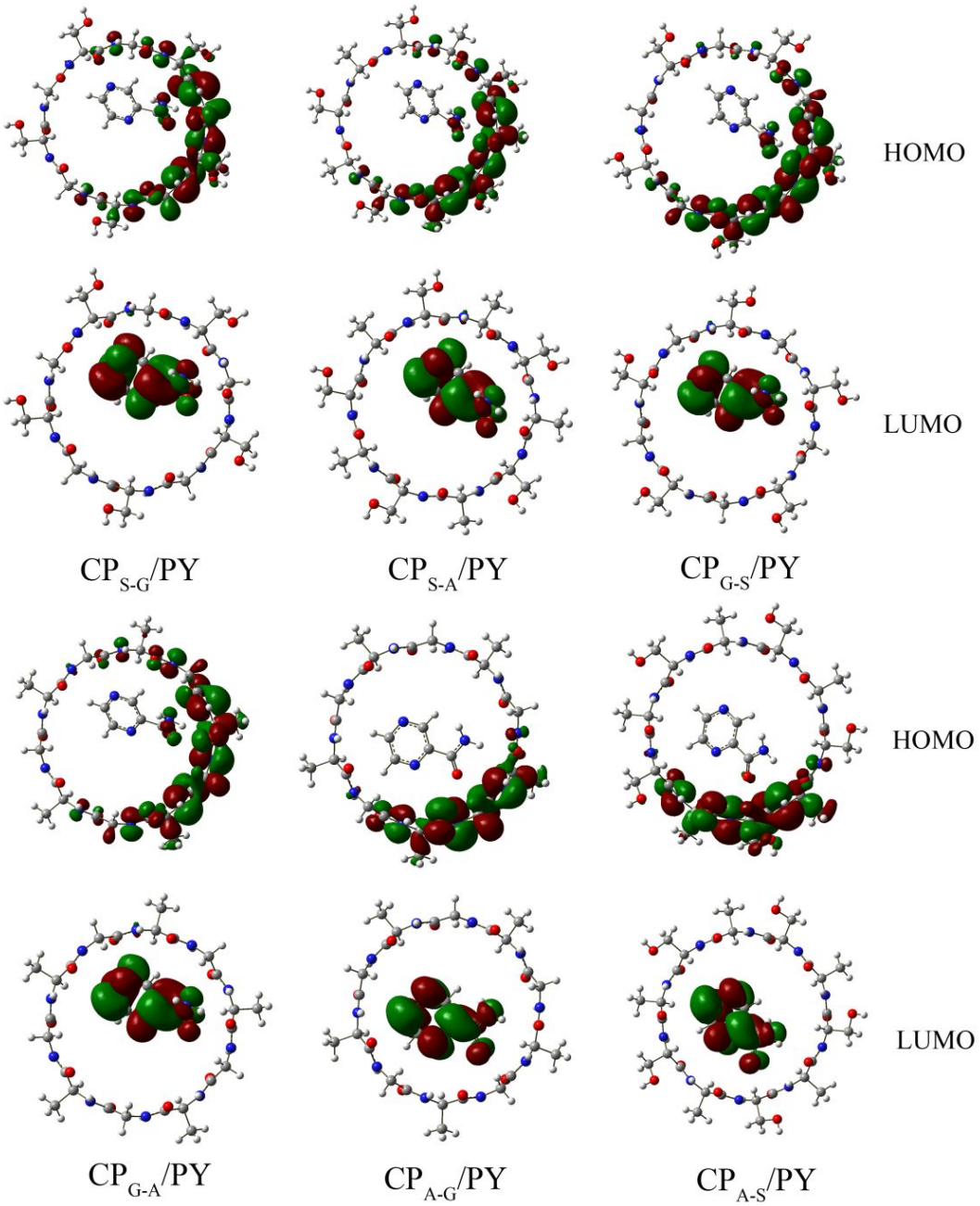

Figure 5. Charge distribution of HOMO and LUMO orbitals for the CP_{X-Y}/PY complexes

As can be seen, in all complexes, the electron density of HOMO is distributed over the cyclic peptide and is mainly placed on the part involved in the interaction, while the LUMO is distributed on the drug. According to Figures 4 and 5, the drug interacts with the HOMO orbitals of the cyclic peptide through its LUMO orbitals. It is predicted that cyclic peptides are more nucleophile, whereas drug molecule is electrophile in nature. The stability of structures depends

View Article Online
DOI: 10.1039/D5NA01168J

on the difference between the energy levels of the HOMO and LUMO orbitals. This difference is called the energy gap. Molecules with higher gap energy are more stable than molecules with lower gap energy. Some of the quantum molecular descriptors for monomers and complexes are given in Table 2.

Table 2 The molecular descriptors for monomers and complexes at the M06-2X/6-31G(d,p)level of theory in the gas phase.

Structure	HOMO(eV)	LUMO(eV)	Eg(eV)	η(eV)	S(eV^{-1})	μ(eV)	ω(eV)	ΔN_{max}(au)	ECT(au)	μ(D)
PY	-8.557	-0.739	7.819	3.909	0.128	-4.648	2.763	0.707		3.41
CPG-G	-8.564	1.363	9.927	4.963	0.101	-3.601	1.306	0.263		0.00
CPA-A	-8.488	1.251	9.739	4.869	0.103	-3.618	1.344	0.276		0.00
CPS-S	-8.080	1.476	9.556	4.778	0.105	-3.302	1.141	0.239		0.00
CPS-A	-8.218	1.274	9.492	4.746	0.105	-3.472	1.270	0.268		1.80
CPS-G	-8.311	1.334	9.645	4.823	0.104	-3.489	1.262	0.262		0.54
CPG-A	-8.523	1.097	9.620	4.810	0.104	-3.713	1.433	0.298		0.42
CP_{G-G}/PY	-8.446	-0.821	7.625	3.812	0.131	-4.634	2.816	0.739	0.476	2.73
CP_{A-A}/PY	-7.880	-0.581	7.299	3.649	0.137	-4.230	2.452	0.672	0.404	3.57
CP_{S-S}/PY	-7.958	-0.297	7.661	3.831	0.131	-4.128	2.224	0.581	0.342	2.45
CP_{S-A}/PY	-8.131	-0.525	7.606	3.803	0.131	-4.328	2.463	0.648	0.380	2.77
CP_{S-G}/PY	-8.174	-0.567	7.607	3.803	0.131	-4.371	2.511	0.660	0.399	2.88
CP_{G-S}/PY	-8.186	-0.542	7.644	3.822	0.131	-4.364	2.492	0.652	0.390	2.92
CP_{G-A}/PY	-8.379	-0.749	7.630	3.815	0.131	-4.564	2.730	0.716	0.418	2.78
CP_{A-G}/PY	-8.132	-0.842	7.290	3.645	0.137	-4.487	2.762	0.758	0.460	3.37
CP_{A-S}/PY	-8.071	-0.771	7.300	3.650	0.137	-4.421	2.677	0.734	0.457	3.37

After the interaction of the PY with cyclic peptides, the HOMO and LUMO states move to lower and higher negative energies, respectively. Due to this change, the energy gap is reduced. This reduction in the energy gap can affect the fluorescence emission of the complexes and aiding in tracking the direction of the drug. The energy gap for CP_{X-Y} structures is lower than that of CP_{X-X} ones. It is predicted that CP_{X-Y}/PY complexes are more reactive than CP_{X-X}/PY complexes, with a greater tendency to interact with drug. The results show that after complexation, the energy gap of CPs decreased, indicating that the interaction of the drug with CPs increases the reactivity of CPs. The energy gap values for complexes are decreased as follows: **CP_{X-X}/PY:** CP_{S-S}/PY> CP_{G-G}/PY> CP_{A-A}/PY; **CP_{X-Y}/PY:** CP_{G-S}/PY> CP_{G-A}/PY> CP_{S-G}/PY> CP_{S-A}PY> CP_{A-S}/PY> CP_{A-G}/PY. The amount of the energy gap for CP_{A-A}/PY and CP_{S-S}/PY complexes is more than that of their corresponding CP_{X-Y}/PY complexes (CP_{A-S}/PY, CP_{A-G}/PY, CP_{S-A}PY, CP_{S-G}/PY). Therefore, the reactivity of CP_{A-A}/PY and CP_{S-S}/PY complexes is less than their corresponding CP_{X-Y}/PY complexes. This result is consistent with the lower interaction energy of

View Article Online
DOI: 10.1039/D5NA01168J

$CP_{A\text{-}A}$/PY and $CP_{S\text{-}S}$/PY complexes compared to the corresponding $P_{X\text{-}Y}$/PY complexes. The opposite of this result was observed in the $CP_{G\text{-}G}$/PY complex. For further investigation, the total density of states (TDOS) and projected density of states (PDOS) diagrams for monomers and complexes are shown in Figure 6. According to the plots, the LUMO and HOMO states shift towards more negative and lower values, respectively, which reduces the energy gap of CPs after interaction with the drug. In these diagrams, CPs and PY have the highest and lowest contributions, respectively.

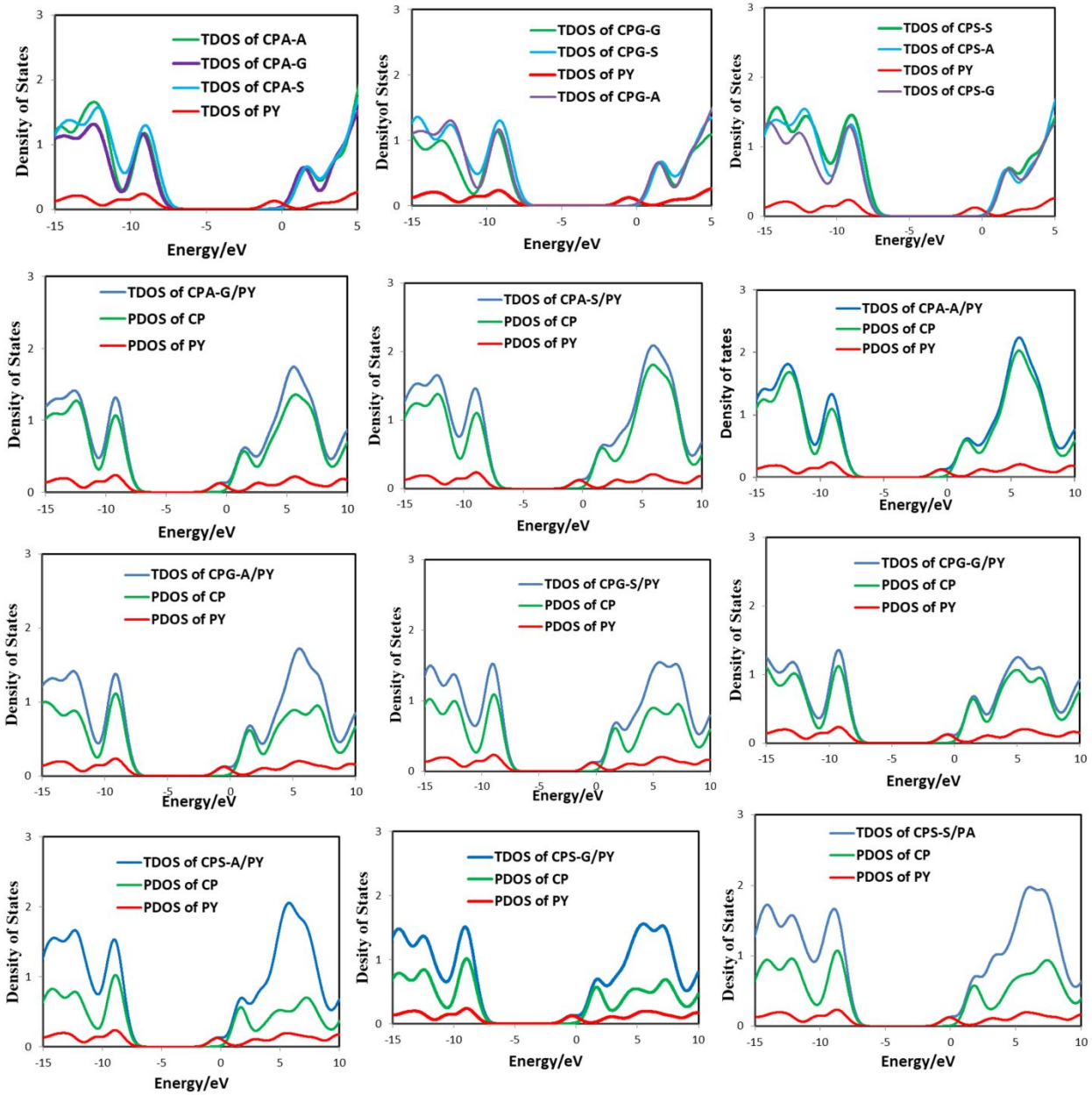

View Article Online
DOI: 10.1039/D5NA01168J

Figure 6. The total and projected density of states for CP_{X-X}/PY and CP_{X-Y}/PY complexes

The reactivity of chemical species could be associated with the molecular descriptors such as electronic chemical potential (μ), hardness (η), softness (S), electrophilicity index (ω), dipole moment (μ), and the maximum charge transfer (ΔN_{max}) (Table 2). As can be seen, these molecular descriptors changed upon complexation. In CP_{X-X}/PY and CP_{X-Y}/PY complexes, the value of η decreases, whereas the value of S, ω, μ, and ΔN_{max} increases upon complexation. Comparison of molecular descriptors in all complexes shows that the values of Eg and η for CP_{A-A}/PY and CP_{S-S}/PY complexes is more than their corresponding CP_{X-Y}/PY complexes (CP_{A-S}/PY, CP_{A-G}/PY, CP_{S-A}PY, CP_{S-G}/PY), in contrast, the values of S, ω, and ΔN_{max} for CP_{A-A}/PY and CP_{S-S}/PY complexes is less than their corresponding CP_{X-Y}/PY complexes. It is predicted that the affinity of CP_{A-A}/PY and CP_{S-S}/PY complexes to the PY drug is less than that of their corresponding CP_{X-Y}/PY complexes. The opposite of this result was observed in the CP_{G-G}/PY complex. From Table 2, the dipole moment of CPs increases upon complexation. The dipole moment of the CP_{X-Y}/PY complexes is more than that in CP_{X-X}/PY complexes. Therefore, cyclic peptides with alternating sequences show a higher affinity for drug interaction in the gas phase. It is predicted that, in a polar solvent, the solubility of CP_{X-Y}/PY complexes is higher than that of CP_{X-X}/PY complexes.

Solvent Effects

Given the vital role of water in the human body, this substance was chosen as the solvent to study the behavior of CP/PY complexes under conditions similar to the biological environment. The interaction energies (ΔE_{sln}), Gibbs free energies of solvation (ΔG^0_{solv}), the energy gap, electronic chemical potential (μ), hardness (η), softness (S), ΔN_{max} and dipole moment for the most stable complexes under water solvent are given in Table 3. All calculations were performed at the M06-2X/6-31G(d,p) level of theory. According to the results, the interaction energies (ΔE_{sln}) of complexes have decreased in water solvent. The ΔE_{sln} value for CP_{S-S}/PY complex is lower than that of their corresponding CP_{X-Y}/PY complexes, indicating that in the solution phase, the affinity of CP_{S-A}/PY and CP_{S-G}/PY complexes to the PY drug is higher than that of the CP_{S-S}/PY complex. The stability order of the CP_{X-Y}/PY complexes is almost similar to that of the gas phase. The negative values of ΔG^0_{Solv} show that the solvation process is spontaneous. Therefore,

View Article Online
DOI: 10.1039/D5NA01168J

the solubility of the system is increased upon complexation. The ΔG^0_{Solv} can be separated in to: $\Delta G^0_{Solv} = \Delta G°_{Solv,elec} + \Delta G°_{Solv,\ nonelec.}$ From Table 3, the contribution of the electrostatic component of ΔG^0_{Solv} is greater than the non-electrostatic component for complexes. Therefore, the electrostatic interactions between the solvent and the solute can lead to changes in the relative energies of the species in water.

Table 3 The electrostatic ($\Delta G^{\circ}_{Solv,ele}$) and Non-electrostatic ($\Delta G^{\circ}_{Solv,nonele}$) contributions to the Gibbs free energy of solvation ($\Delta G°_{solv}$), the interaction energy in solution (ΔE_{sln}), dipole moment (D), and the molecular descriptors for most sable complexes at the M06-2X/6-31G(d,p) level of theory in the solution phase.

Structure	ΔE_{Sln}	ΔG^0_{Solv}	$\Delta G^0_{Solv,elec}$	$\Delta G^0_{Solv,non-elec}$	μ(D)	Eg(eV)
CP_{S-S}/PY	-55.97	-62.48	-83.5	21.02	3.25	7.858
CP_{S-G}/PY	-78.64	-80.73	-96.61	15.88	7.83	7.728
CP_{S-A}/PY	-62.59	-77.71	-97.62	19.91	5.23	7.724
Structure	**η(eV)**	**S(eV^{-1})**	**μ(eV)**	**ω(eV)**	**ΔN_{max}(au)**	
CP_{S-S}/PY	3.929	0.12726	-4.622	2.719	0.692	
CP_{S-G}/PY	3.864	0.12940	-4.605	2.745	0.710	
CP_{S-A}/PY	3.862	0.12946	-4.608	2.749	0.712	

The value of the dipole moment of complexes in the solution phase shows that the dipole moment of the complexes has increased in going from the gas phase to the solution phase. Therefore, the dipole moment of the complexes increases after dissolution. Examination of the results in Table 3 show that the values of Eg and η for CP_{S-A}/PY and CP_{S-G}/PY complexes is less than CP_{S-S}/PY complex, in contrast, the values of S, ω, and ΔN_{max} for CP_{S-A}/PY and CP_{S-G}/PY complexes is more than CP_{S-S}/PY complex. These results are consistent with the gas phase results. Comparison of the solution-phase data shows that in the CP_{S-S}/PY complex, the energy gap, chemical hardness, chemical potential, electrophilicity index, and ΔN_{max} decreased, while softness increased compared to the gas phase. The opposite trend is observed for the CP_{S-A}/PY and CP_{S-G}/PY complexes.

NBO, AIM, ELF, and RDG analysis

In this work, the electron density transfers are investigated using NBO analysis. The results of the NBO analysis at M06-2X/6-31G(d,p) level of theory are reported in Table 1. Non-covalent interactions between species lead to changes in the sum of their atomic charges. After

View Article Online
DOI: 10.1039/D5NA01168J

complexation, the sum of the atomic charges of CPs and drug atoms changes, indicating that charge transfer (CT) occurs between the PY and CP. The charge transfer can be defined as the sum of atomic charges on a drug. The results show that, in all complexes, the charge transfers occur from the CP to PY. The amount of charge transfer in $CP_{X\text{-}Y}$/PY complexes is more than that of $CP_{X\text{-}X}$/PY complexes. This result is consistent with the higher interaction energy and higher affinity of $CP_{X\text{-}Y}$/PY complexes with the drug than $CP_{X\text{-}X}$/BNNT complexes. Investigations show that an alternating sequence of amino acids increases the charge transfer between the drug and the CP. In the $CP_{X\text{-}Y}$/PY complexes, strong interactions between the drug and the cyclic peptide enhance the charge transfer from the cyclic peptide to the drug. In each class of $CP_{X\text{-}Y}$/PY structures, a quantitative correlation is observed between the interaction energy and the charge transfer rate, such that structures with higher interaction energy show higher charge transfer rates. This trend indicates that increasing the interaction strength enhances electron redistribution, which is expected to improve the stability of the drug-carrier complex. Small values of charge transfer for non-covalent interactions indicate that no covalent bond is formed and the reversible nature of the carrier-drug interaction is maintained. Also, the data trend shows that a small increase in charge transfer is positively correlated with the enhancement of the interaction energy (ΔE_{int}).

The quantum theory of atoms in molecules (QTAIM) was used to determine the nature of interactions. In this study, to determine the nature of the interactions between cyclic peptides and the PY drug, AIM analysis was performed at M06-2X/6-31G(d,p) level of theory. The molecular graphs indicating the bond critical points (BCPs) and bond paths for $CP_{X\text{-}X}$/PY complexes are shown in Figure 7. In all complexes, the molecular graphs represent additional critical points in the intermolecular regions.

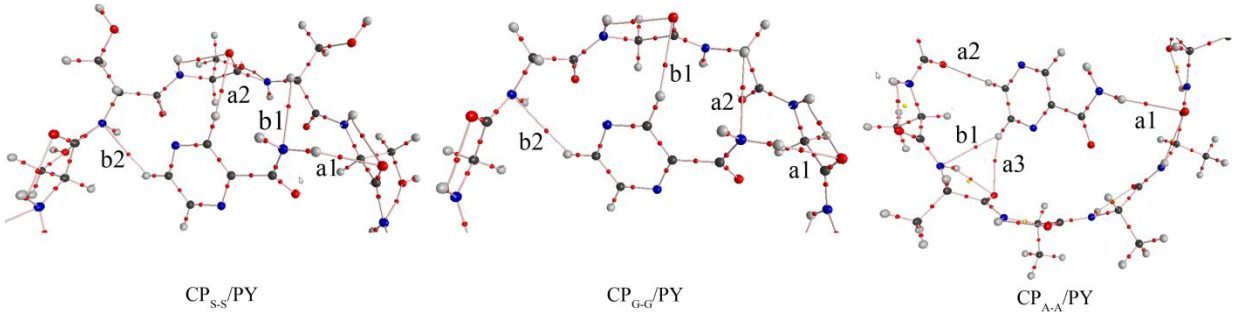

Figure 7. Molecular graphs for $CP_{X\text{-}X}$/PY complexes at M06-2X/6-31G(d,p) level of theory

View Article Online
DOI: 10.1039/D5NA01168J

The values of electron density, ρ(r), the electron density Laplacian, $\nabla^2\rho(r)$, total electronic energy density, H(r), at O…H and N…H bond critical points (BCPs) of complexes are reported in Table 4.

Table 4 Calculated BCPs data (au) for $CP_{X\text{-}X}$/PY and $CP_{X\text{-}Y}$/PY complexes at M06-2X/6-31G(d,p) level of theory.

Bond	ρ(r)	$\nabla^2\rho(r)$	H(r)	ρ(r)	$\nabla^2\rho(r)$	H(r)	ρ(r)	$\nabla^2\rho(r)$	H(r)
		$CP_{A\text{-}A}$/PY			**$CP_{G\text{-}G}$/PY**			**$CP_{S\text{-}S}$/PY**	
$(O\ldots H)_{a1}$	0.0105	0.0336	0.0077	0.0192	0.0583	0.0157	0.0194	0.0594	0.0160
$(O\ldots H)_{a2}$	0.0096	0.0304	0.0065	0.0100	0.0327	0.0068	0.0102	0.0331	0.0070
$(O\ldots H)_{a3}$	0.0058	0.0204	0.0034	-	-	-	-	-	-
$(N\ldots H)_{b1}$	0.0081	0.0248	0.0048	0.0063	0.0197	0.0035	0.0065	0.0199	0.0036
$(N\ldots H)_{b2}$	-	-	-	0.0081	0.0256	0.0049	0.0077	0.0248	0.0046
		$CP_{A\text{-}G}$/PY			**$CP_{G\text{-}A}$/PY**			**$CP_{S\text{-}G}$/PY**	
$(O\ldots H)_{a1}$	0.0106	-0.0085	0.0078	0.0195	0.0599	0.0161	0.0197	0.0599	0.0162
$(O\ldots H)_{a2}$	0.0094	-0.0074	0.0063	0.0099	0.0325	0.0067	0.0104	0.0339	0.0072
$(O\ldots H)_{a3}$	0.0059	-0.0052	0.0035	-	-	-	-	-	-
$(N\ldots H)_{b1}$	0.0082	-0.0063	0.0049	0.0061	0.0189	0.0033	0.0069	0.0213	0.0038
$(N\ldots H)_{b2}$	-	-	-	0.0079	0.0251	0.0048	0.0079	0.0254	0.0047
		$CP_{A\text{-}S}$/PY			**$CP_{G\text{-}S}$/PY**			**$CP_{S\text{-}A}$/PY**	
$(O\ldots H)_{a1}$	0.011	0.03516	0.00833	0.0195	0.0588	0.0159	0.0196	0.0588	0.0159
$(O\ldots H)_{a2}$	0.009	0.02963	0.00622	0.0104	0.0336	0.0072	0.0101	0.033	0.0069
$(O\ldots H)_{a3}$	0.005	0.0194	0.00316	-	-	-	-	-	-
$(N\ldots H)_{b1}$	0.008	0.0244	0.00482	0.0067	0.0205	0.0037	0.0061	0.0189	0.0033
$(N\ldots H)_{b2}$	-	-	-	0.0079	0.0253	0.0047	0.008	0.0255	0.0048

The results show that the electron densities at O…H interactions are greater than those of at N…H ones that are in agreement with the smaller O…H distance in comparison with the N…H ones. Thus, it is predicted that in all complexes, O…H interactions are stronger than N…H ones. Comparison of ρ(r) values shows that the ρ(r) value corresponding to the shortest interaction $(O\ldots H)_a$ in $CP_{X\text{-}Y}$/PY complexes is higher than its value in $CP_{X\text{-}X}$/PY complexes. This result is consistent with the shorter distance of this interaction in $CP_{X\text{-}Y}$/PY complexes compared to $CP_{X\text{-}X}$/PY complexes. The values of $\nabla^2\rho(r)$ and H(r) at hydrogen bond critical points in all the complexes are positive. Therefore, values of $\nabla^2\rho(r)$ and H(r) indicate that all H-bonds have electrostatic nature.

View Article Online
DOI: 10.1039/D5NA01168J

The RGD analysis is used to investigate the strength of interactions in intermolecular regions. The reduced density gradient (RDG) is a scalar field of the electron density (ρ) that can be defined as:

$$\mathrm{RDG}(r) = \frac{|\nabla\rho(r)|}{2(3\pi^2)\rho(r)^{4/3}} \quad (9)$$

where, ρ(r) and ∇ρ(r) are the electron density and its first derivative, respectively [59]. In these diagrams, the attractive, van der Waals, and repulsive interactions are marked with blue, green, and red colors, respectively. The RDG plots for the optimized complexes are displayed in Figure 8.

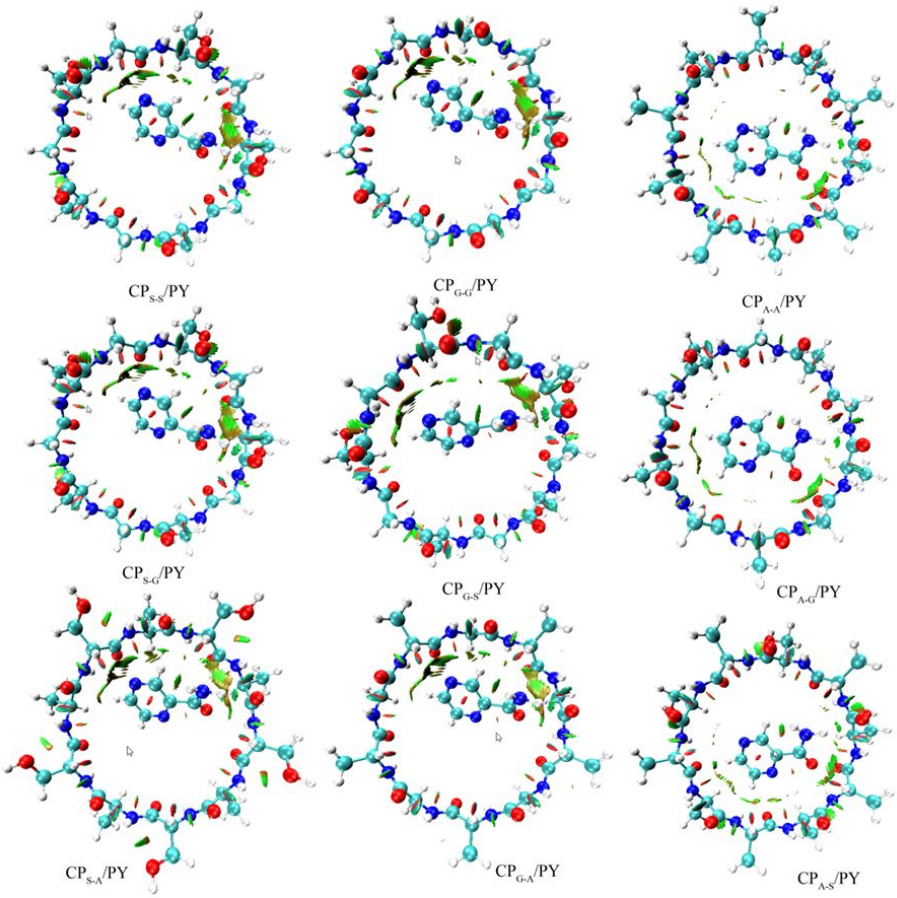

Figure 8. The RDG map for the optimized complexes

View Article Online
DOI: 10.1039/D5NA01168J

In RDG plots, the areas between drug and the cyclic peptides are mainly marked with green and brown color isosurfaces, which show that the interactions are the type of non-covalent and vdW. Van der Waals interactions refer to weak non-covalent interactions, including hydrogen bonding, with electrostatic dominance. These non-covalent interactions are confirmed by the independent gradient model (IGM) and δg descriptive function. The IGM analysis allows separating the δg as δg^{inter} and δg^{intra}, which solely reflect the contribution to δg due to inter-fragment (non-covalent) and intra-fragment (covalent) interactions, respectively. According to the IGM-δg scattered map of different complexes, inter-fragment or intra-fragment interactions are shown in Figure 9. The red and black scattered points correspond to δg^{inter} and δ^{gintra} fragments interactions, respectively. In the region where sign(λ2)ρ is about -0.04, it can be seen that the δ^{ginter} has a remarkable peak (With a height of nearly 0.05), which implies the presence of hydrogen bonds.

View Article Online
DOI: 10.1039/D5NA01168J

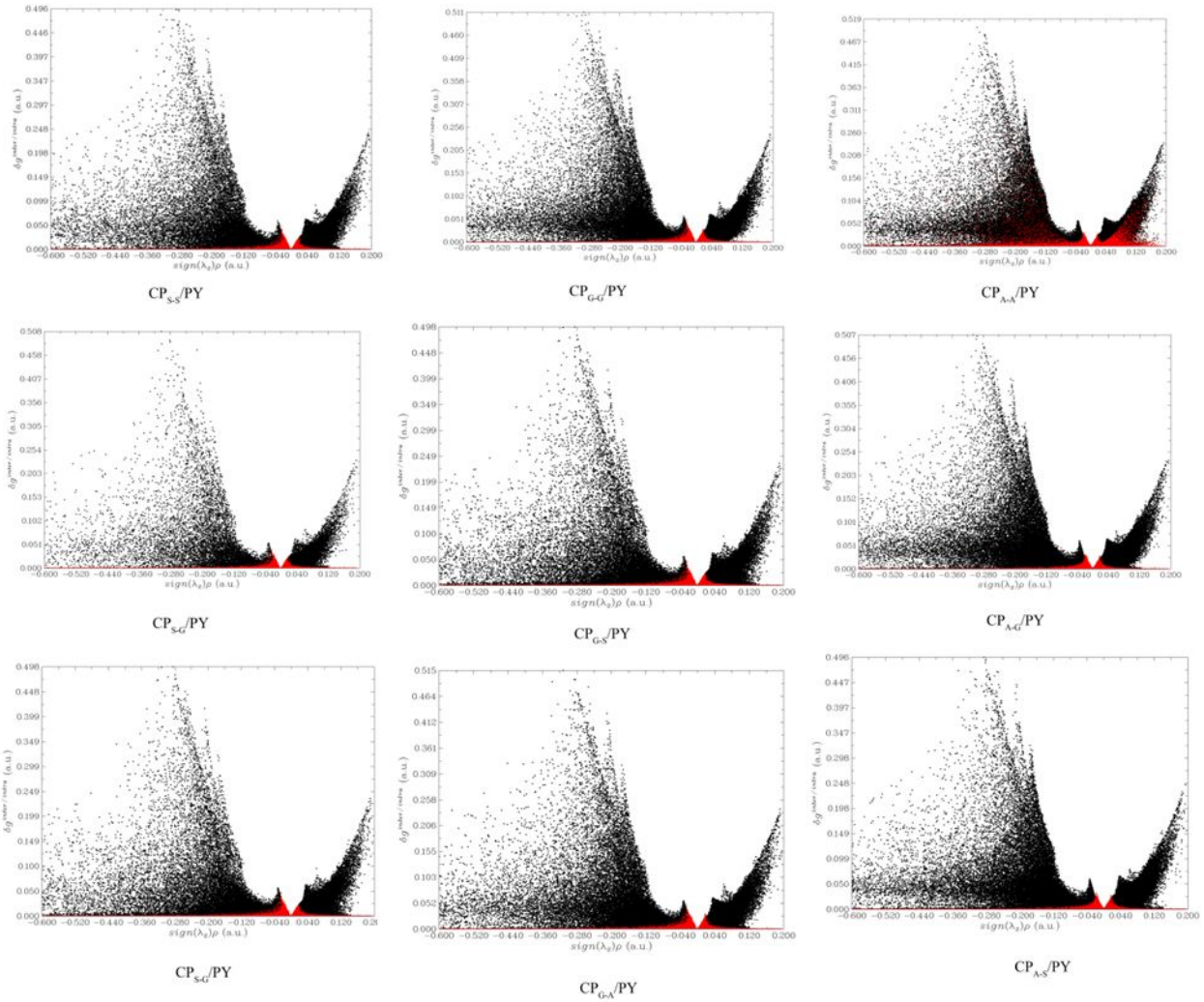

Figure 9. Independent Gradient Model (IGM) of PY on $CP_{X\text{-}X}$/PY and $CP_{X\text{-}Y}$/PY complexes.

In the continuation of work, ELF (electron localization function) maps for all complexes were plotted using Multiwfn and are shown in Figure 10.

View Article Online
DOI: 10.1039/D5NA01168J

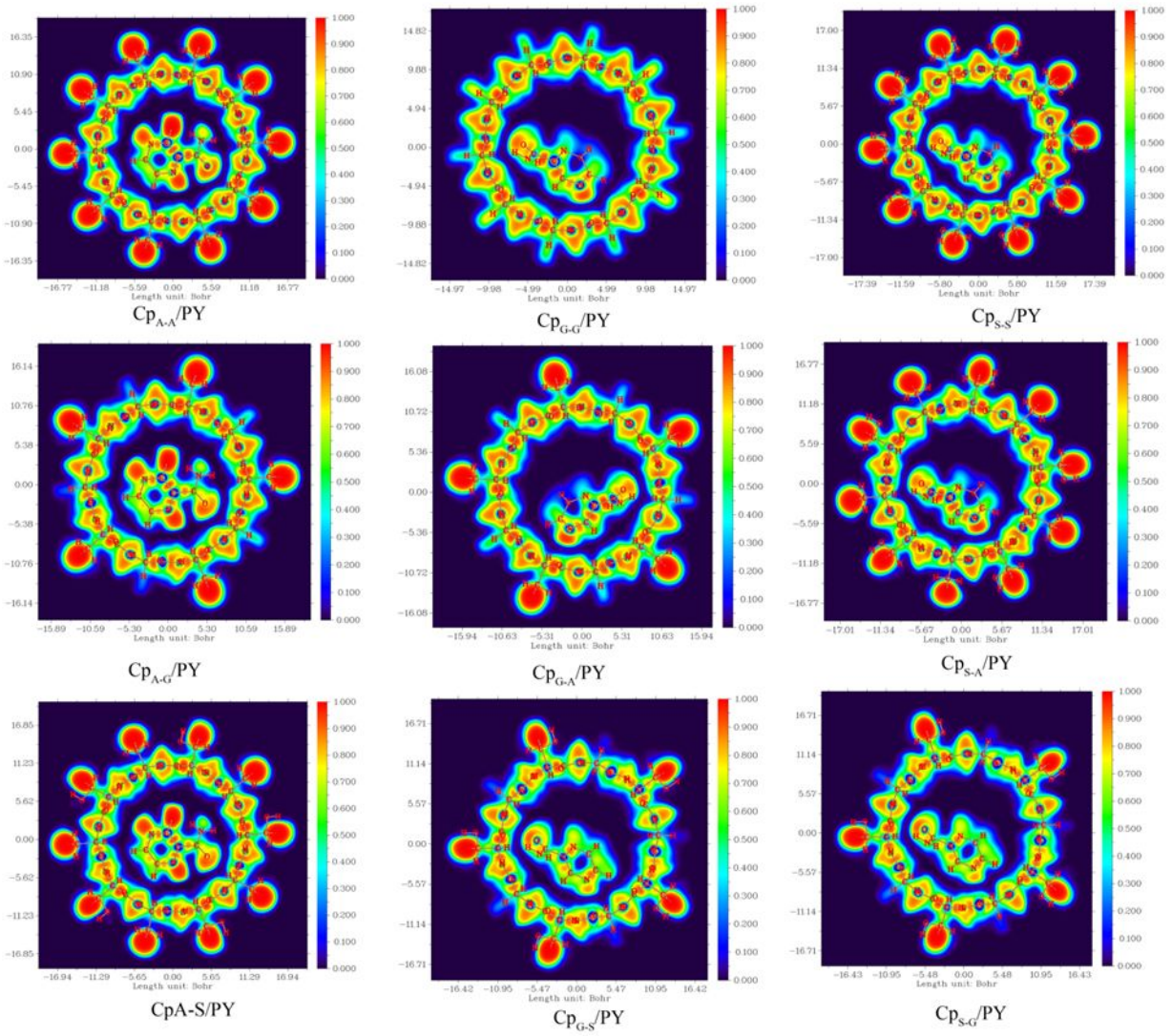

Figure 10. ELF maps of the interaction of the PY drug with cyclic peptides

This map represents the homogeneous Jellium-like electron gas model; the values are normalized between 0.0 and 1.0. The red regions indicate extreme localization (value 1.0). The green regions indicate a free electron gas behavior (value 0.5), and the blue regions indicate non-localization (value 0.0). The presence of these colored regions between the drug and the cyclic peptide indicates electron localization between the drug and the cyclic peptide. Figure 10 shows relatively strong electron localization between the NH_2CO group of drug and the cyclic peptide ring (yellow color). It indicates that the interactions are stronger in this region.

View Article Online
DOI: 10.1039/D5NA01168J

The results of this study provide an electronic and structural basis for understanding the effect of amino acid sequence in cyclic peptides on the interaction with pyrazinamide. Therefore, this is the first step towards the rational design of drug carriers. In the next step, other properties of the structures, including thermal stability, toxicity, drug release, membrane permeability, and bioavailability, should be evaluated in in vivo studies.

Conclusion

This research focuses on investigating the interaction of anti-tuberculosis drug PY with the cyclic decapeptides of Glycine(G), Alanine(A), and Serine(S) and their binary alternating sequences at the M06-2X/6-31G(d,p) level of theory in the gas and solution phases. So we are dealing with two types of complexes $CP_{X\text{-}X}$/PY($CP_{S\text{-}S}$/PY, $CP_{G\text{-}G}$/PY, $CP_{A\text{-}A}$/PY) and $CP_{X\text{-}Y}$/PY($CP_{S\text{-}A}$/PY, $CP_{S\text{-}G}$/PY, $CP_{G\text{-}S}$/PY, $CP_{G\text{-}A}$/PY, $CP_{A\text{-}G}$/PY, $CP_{A\text{-}S}$/PY). In the obtained complexes, two types of hydrogen bonds, O...H and N...H, were observed. It seems that hydrogen bonds formed between the drug and cyclic peptides play an important role in the stability of the complexes. Comparison of the two types of hydrogen bonds in the complexes shows that the O...H hydrogen bonds are shorter than the N...H bonds. On the other hand, the O...H interactions observed in $CP_{X\text{-}Y}$/PY complexes are shorter than those in $CP_{X\text{-}X}$/PY complexes. Hence, in $CP_{X\text{-}Y}$/PY complexes, the absolute value of E_{HB}($|E_{HB}|$) related to O…H hydrogen bond is greater than that of $CP_{X\text{-}X}$/PY complexes. Examination of the energy results shows that the affinity of $CP_{X\text{-}Y}$/PY complexes for drug interaction is higher than that of $CP_{X\text{-}X}$/PY complexes. Thus, it is predicted the interactions in $CP_{X\text{-}Y}$/PY complexes be stronger than $CP_{X\text{-}X}$/PY complexes. The hydrogen interactions in the complexes are of the Van der Waals type. Therefore, PY drug can physically interact with the cyclic peptides. The value of the dipole moment for $CP_{X\text{-}Y}$/PY complexes is more than $CP_{X\text{-}X}$/PY complexes, indicating that the polarity of $CP_{X\text{-}Y}$/PY complexes is more than $CP_{X\text{-}X}$/PY complexes. The energy gap values for the $CP_{A\text{-}A}$/PY and $CP_{S\text{-}S}$/PY complexes are more than those for the $CP_{X\text{-}Y}$/PY complexes. Therefore, the affinity of $CP_{A\text{-}A}$/PY and $CP_{S\text{-}S}$/PY complexes to the PY drug is less than that of their corresponding $CP_{X\text{-}Y}$/PY complexes. This result is also observed for the most stable complex in the solution phase. The dipole moment value of the complexes in the solution phase has increased compared to the gas phase. In all complexes, the charge transfer takes place from the cyclic peptide to the drug. The amount of charge transfer in $CP_{X\text{-}Y}$/PY complexes is more than

View Article Online
DOI: 10.1039/D5NA01168J

CP_{X-X}/PY. Structures with higher interaction energy show higher charge transfer rates. Based on the AIM analysis, the electron density ρ(r) at O…H BCPs for CP_{X-Y}/PY complexes is more than that of the CP_{X-X}/PY complexes, which corresponds to the higher interaction energy in these structures. This result is in agreement with the shorter O...H hydrogen bond distances in the CP_{X-Y}/PY complexes compared to CP_{X-X}/PY ones. The nature of the O…H and N…H interactions in all complexes is electrostatic. Finally, the alternating sequence of amino acids in cyclic peptides increases the stability of the structures and improves their properties. Hence, the affinity of CP_{X-Y}/PY complexes for interaction with PA is stronger than that of CP_{X-X}/PY complexes.

Conflicts of interest

All authors declare that they have no conflicts of interest.

Data Availability Statement:

Data available on request from the authors.

References

(1) Jamroży, M.; Kudłacik-Kramarczyk, S.; Drabczyk, A.; Krzan, M. Advanced drug carriers: a review of selected protein, polysaccharide, and lipid drug delivery platforms. *Int. J. Mol. Sci.* **2024**, *25* (2), 786.

(2) Khudhair, A. M.; Ahmed, A. B.; Ajeel, F. N. Computational Investigation of 6-Thioguanine Adsorption on Armchair Graphene Nanoribbons for Targeted Drug Delivery: Orientation-Dependent Stability, Electronic Structure, and Delivery Efficiency, *J. Phys. Chem. C.* **2025**, 129, 16593−16603.

(3) Khudhair, A. M.; Dhouib, I.; Ahmed, A. B.; Ajeel, F. N.; Khemakhem, B. DFT-based insights into cisplatin drug adsorption on transition metal dichalcogenides: toward targeted drug delivery systems, *Chinese Journal of Physics*. **2025**, 97, 827–838.

View Article Online
DOI: 10.1039/D5NA01168J

(4) Naderi, F.; Veryazov, V. Multiconfigurational Study of the Electronic Structure of Negatively Charged Fullerens. *J. Chem.* **2017**, *11*, 30–36.

(5) Khudhair, A. M.; Dhouib, I.; Ajeel, F. N.;·Ahmed, A. B.; Khemakhem, B. A Novel $A_{l8}N_8$ and B_8N_8 Nanoring Monolayer for Sensing and Drug Delivery of Cisplatin and Nitrosourea Anticancer Drugs: A DFT Insight, *J. Inorg. Organomet. Polym. Mater*. **2025**, 35, 7593–7606

(6) Ghasemi, A. S.; Makiabadi, B.; Zakarianezhad, M.; Soltani, A.; Ashrafi, F.; Mashhadban, F. Experimental and theoretical studies of the interaction of Penicillamine with SWCNT (6, 0) as a drug delivery system. *Inorg. Nano-Met. Chem.* **2024**, *54* (6), 525–533.

(7) Makiabadi, B.; Zakarianezhad, M.; Zeydabadi, E. The role of hydrogen bonds on the stability of anticancer drug compounds TG/uracil, TG/5-fluorouracil and TG/gimeracil. *Struc. Chem.* **2023**, *34* (3), 755–767.

(8) Naderi, F.; Veryazov, V. The electronic structure of negatively charged fullerenes: From monomers to dimers. *Comput. Methods Sci. Eng.* **2017,** *1906* (1), 030024.

(9) Makiabadi, B.; Naderi, F.; Zakarianezhad, M. Theoretical investigation of Diels–Alder reaction mechanism and regioselectivity with functionalized fullerene derivatives. *J. Chin. Chem. Soc.* **2024**, *71* (12), 1418–1426.

(10) Bardan, K. H.; Ajeel, F. N.; Mohammed, M. H.; Khudhair, A. M.; Ahmed, A. B. DFT study of adsorption properties of the ammonia on both pristine and Si-doped graphene nanoflakes, *Chem. Phys. Impact*. **2024**, 8, 100561.

(11) Khudhair, A. M.; Ahmed, A. B.; Ajeel, F. N.; Mohammed, M. H. Theoretical investigation on the therapeutic applications of C2B and C2O as targeted drug delivery systems for hydroxyurea and 6-thioguanine in cancer treatment, *Nano-Structures&Nano-Objects.* **2024***,* 38, 101135

(12) Khoshbayan, B.; Morsali, A.; Beyramabadi, S. A.; Bozorgmehr, M. R. DFT-QTAIM Study of Gold Nanoparticles and Cyclic Peptide as Effective Drug Nanocarriers. Orbital: *Electron. J. Chem.* **2020**, *12*(3), 160–171.

(13) Nasrolahi Shirazi, A.; Mandal, D.; Tiwari, R. K.; Guo, L.; Lu, W.; Parang, K. Cyclic peptide-capped gold nanoparticles as drug delivery systems. Mol. Pharm. **2013**, *10* (2), 500–511.

View Article Online
DOI: 10.1039/D5NA01168J

(14) Ramadhani, D.; Maharani, R.; Gazzali, A. M.; Muchtaridi, M. Cyclic peptides for the treatment of cancers: A review. *Molecules* **2022**, *27* (14), 4428.

(15) Tyler, T. J.; Durek, T.; Craik, D. J. Native and engineered cyclic disulfide-rich peptides as drug leads. *Molecules* **2023**, *28* (7), 3189.

(16) Oh, D.; Darwish, S. A.; Shirazi, A. N.; Tiwari, R. K.; Parang, K. Amphiphilic bicyclic peptides as cellular delivery agents. *Chem. Med. Chem.* **2014**, *9* (11), 2449–2453.

(17) Dougherty, P. G.; Sahni, A.; Pei, D. Understanding cell penetration of cyclic peptides. *Chem. Rev.* **2019**, *119* (17), 10241–10287.

(18) Nasrolahi Shirazi, A.; Salem El-Sayed, N.; Kumar Tiwari, R.; Tavakoli, K.; Parang, K. Cyclic peptide containing hydrophobic and positively charged residues as a drug delivery system for curcumin. *Curr. Drug. Delv.* **2016**, *13* (3), 409–417.

(19) Remesic, M.; Sun Lee, Y.; J Hruby, V. Cyclic opioid peptides. *Curr. Med. Chem.* **2016**, *23* (13), 1288–1303.

(20) Martian, P. C.; Tertis, M.; Leonte, D.; Hadade, N.; Cristea, C.; Crisan, O. Cyclic peptides: A powerful instrument for advancing biomedical nanotechnologies and drug development. *J. Pharm. Biomed. Anal.* **2025**, *252*, 116488.

(21) Ji, X.; Nielsen, A. L.; Heinis, C. Cyclic peptides for drug development. *Angew. Chem.* **2024**, *136* (3), e202308251.

(22) Jagrosse, M. L.; Baliga, U. K.; Jones, C. W.; Russell, J. J.; García, C. I.; Najar, R. A.; Rahman, A.; Dean, D. A.; Nilsson, B. L. Impact of peptide sequence on functional siRNA delivery and gene knockdown with cyclic amphipathic peptide delivery agents. *Mol. Pharm.* **2023**, *20* (12), 6090–6103.

(23) Hsieh, W.-H.; Liaw, J. Applications of cyclic peptide nanotubes (cPNTs).*J. F. Drug. Anal.* **2019**, *27* (1), 32–47.

(24) Park, S. E.; Sajid, M. I.; Parang, K.; Tiwari, R. K. Cyclic cell-penetrating peptides as efficient intracellular drug delivery tools. *Mol. Pharm.* **2019**, *16* (9), 3727–3743.

View Article Online
DOI: 10.1039/D5NA01168J

(25) Wang, C.; Shen, Z.; Chen, Y.; Wang, Y.; Zhou, X.; Chen, X.; Li, Y.; Zhang, P.; Zhang, Q. Research progress on cyclic-peptide functionalized nanoparticles for tumor-penetrating delivery. *Int. J. Nanomedicine* **2024**, 12633–12652.

(26) Fakhari, S.; Nouri, A.; Jamzad, M.; Arab-Salmanabadi, S.; Falaki, F. Investigation of inclusion complex of metformin into selective cyclic peptides as novel drug delivery system: Structure, electronic properties, AIM, and NBO study via DFT. *J. Chin. Chem. Soc.* **2021**, *68* (1), 67–75.

(27) Morsali, A.; Momen Heravi, M.; Beyramabadi, S. A. Selenium-capped cyclic peptide nanoparticles for penicillamine drug delivery: A DFT Study. *Indian J. Chem.-Inorg. Phys. Theor. Anal. Chem.* **2020**, *59* (1), 43–50.

(28) Pham, D.-D.; Fattal, E.; Tsapis, N. Pulmonary drug delivery systems for tuberculosis treatment. *Int. J. Pharm.* **2015**, *478* (2), 517–529.

(29) Chandila, S.; Kaushik, H. Current trends and challenges in tuberculosis: A systemic review. *World J. Pharm. Res.* **2023**, *12*, 355–367.

(30) Santucci, P.; Greenwood, D. J.; Fearns, A.; Chen, K.; Jiang, H.; Gutierrez, M. G. Intracellular localisation of Mycobacterium tuberculosis affects efficacy of the antibiotic pyrazinamide. *Nat. Commun.* **2021**, *12* (1), 3816.

(31) Moumivand, A.; Naderi, F.; Moradi, O.; Makiabadi, B. Smart drug delivery: a DFT study of C24 fullerene and doped analogs for pyrazinamide. *Nanoscale. Adv.* **2025**, *7* (5), 1287–1299.

(32) Omoteso, O. A.; Fadaka, A. O.; Walker, R. B.; Khamanga, S. M. Innovative Strategies for Combating Multidrug-Resistant Tuberculosis: Advances in Drug Delivery Systems and Treatment. *Microorganisms* **2025**, *13* (4), 722.

(33) Clemens, D. L.; Lee, B.-Y.; Xue, M.; Thomas, C. R.; Meng, H.; Ferris, D.; Nel, A. E.; Zink, J. I.; Horwitz, M. A. Targeted intracellular delivery of antituberculosis drugs to Mycobacterium tuberculosis-infected macrophages via functionalized mesoporous silica nanoparticles. *Antimicrob. Agents Chemother.* **2012**, *56* (5), 2535–2545.

View Article Online
DOI: 10.1039/D5NA01168J

(34) Gelperina, S.; Kisich, K.; Iseman, M. D.; Heifets, L. The potential advantages of nanoparticle drug delivery systems in chemotherapy of tuberculosis. *Am. J. Respir. Crit. Care. Med.* **2005**, *172* (12), 1487–1490.

(35) Arnab, S. R.; Halder, J.; Islam, M. S. MoSe2 and Al-Doped MoSe2 as targeted carriers for anti-tuberculosis drug delivery with controlled release: A first-principles DFT study. *Inorg. Chem. Commun.* **2025**, *174*, 113979.

(36) Sharma, A.; Sharma, S.; Khuller, G. Lectin-functionalized poly (lactide-co-glycolide) nanoparticles as oral/aerosolized antitubercular drug carriers for treatment of tuberculosis. *J. Antimicrob. Chemother.* **2004**, *54* (4), 761–766.

(37) Rojanarat, W.; Nakpheng, T.; Thawithong, E.; Yanyium, N.; Srichana, T. Levofloxacin-proliposomes: opportunities for use in lung tuberculosis. *Pharmaceutics* **2012**, *4* (3), 385–412.

(38) Li, C.; Wang, Y.; Zhang, X.; Deng, L.; Zhang, Y.; Chen, Z. Tumor-targeted liposomal drug delivery mediated by a diseleno bond-stabilized cyclic peptide. *Int. J. Nanomedicine.* **2013**, 1051–1062.

(39) Buya, A. B.; Witika, B. A.; Bapolisi, A. M.; Mwila, C.; Mukubwa, G. K.; Memvanga, P. B.; Makoni, P. A.; Nkanga, C. I. Application of lipid-based nanocarriers for antitubercular drug delivery: a review. *Pharmaceutics.* **2021**, 13 (12), 2041.

(40) Kumar, M.; Virmani, T.; Kumar, G.; Deshmukh, R.; Sharma, A.; Duarte, S.; Brandão, P.; Fonte, P. Nanocarriers in tuberculosis treatment: challenges and delivery strategies. *Pharmaceuticals* **2023**, *16* (10), 1360.

(41) Pandurangan, K.; Roy, B.; Rajasekhar, K.; Suseela, Y. V.; Nagendra, P.; Chaturvedi, A.; Satwik, U. R.; Murugan, N. A.; Ramamurty, U.; Govindaraju, T. Molecular architectonics of cyclic dipeptide amphiphiles and their application in drug delivery. *ACS Appl. Bio Mater.* **2020**, *3* (5), 3413–3422.

(42) Saikia, N.; Rajkhowa, S.; Deka, R. C. Density functional and molecular docking studies towards investigating the role of single-wall carbon nanotubes as nanocarrier for loading and delivery of pyrazinamide antitubercular drug onto pncA protein. *J Comput Aided Mol Des*. **2013**, 27 (3), 257

View Article Online
DOI: 10.1039/D5NA01168J

(43) Shahabi, M.; Raissi, Heidar. Assessment of solvent effects on the inclusion behavior of pyrazinamide drug into cyclic peptide based nanotubes as novel drug delivery vehicles. *J. Mole. Liq*. **2018**, 268, 326.

(44) Chou-Yi, H.; Mutar, A. A.; Ameer, A.J.; Kadhim, M. M.; Hamza, T. A.; ALsailawi, H.A.; Altimari, U. S.; Alawadi, Ahmed.; Alsalamy, A. Exploring boron nitride nanostructures for effective pyrazinamide drug delivery: A DFT study. *Comput. Theor. Chem*. **2023**, 1230, 114378

(45) Frisch, M. gaussian 09, Revision d. 01, Gaussian. *Inc, Wallingford CT* **2009**, *201*.

(46) Boys, S. F.; Bernardi, F. The calculation of small molecular interactions by the differences of separate total energies. Some procedures with reduced errors. *Mol. Phys*. **1970**, *19* (4), 553–566.

(47) Padmanabhan, J.; Parthasarathi, R.; Subramanian, V.; Chattaraj, P. Electrophilicity-based charge transfer descriptor. *J. Phys. Chem. A*. **2007**, *111* (7), 1358–1361.

(48) Miertus, S.; Scrocco, E. Electrostatic interaction of a solute with a continuum. A direct utilizaion ofAB initiomolecular potentials for the prevision of solvent effects. *J Chem Phys*. **1981**, 55,117–129

(49) Silvi, B.; Savin, A. Classification of chemical bonds based on topological analysis of electron localization functions. *Nature* **1994**, *371* (6499), 683–686.

(50) Lu, T.; Chen, F. Multiwfn: A multifunctional wavefunction analyzer. *J. Comput. Chem.* **2012**, *33* (5), 580–592.

(51) Reed, A. E.; Curtiss, L. A.; Weinhold, F. Intermolecular interactions from a natural bond orbital, donor-acceptor viewpoint. *Chem. Rev.* **1988**, *88* (6), 899–926.

(52) Biegler-Konig, F.; Schonbohm, J.; Bayles, D. Software news and updates-AIM2000-A program to analyze and visualize atoms in molecules. *J. Comput. Chem.* **2001**, *22* (5), 545.

(53) Ektefa, F.; Khodadadi, Z.; Naderi, F.; Fathi, F. A computational evidence of the intermolecular hydrogen bonding in leflunomide: Chemical shielding tensors. *Comput. Theor. Chem.* **2023**, *1221*, 114027.

View Article Online
DOI: 10.1039/D5NA01168J

(54) Masoodi, H. R.; Zakarianezhad, M.; Bagheri, S.; Makiabadi, B.; Shool, M. Substituent effects on some calculated NMR data in T-shaped configuration of benzene dimer. *Chem.l Phys. Lett.* **2014**, *614*, 143–147.

(55) Bagheri, S.; Masoodi, H. R.; Mohammadi, M.; Zakarianezhad, M.; Makiabadi, B. The influence of number of nitrogen atoms on the NMR data in aromatic azine⋯ HF complexes. *Chem. Phys. Lett.* **2013**, *572*, 26–31.

(56) Makiabadi, B.; Zakarianezhad, M.; Behjatmanesh-Ardakani, R.; Mousavi, S. H. Investigating the performance of BN nanotubes as drug delivery systems for Azacitidine and Decitabine anti-cancer drugs: A theoretical study. *Comput. Theor. Chem.* **2024**, *1231*, 114429

(57) Hadipour, N. L.; Ahmadi Peyghan, A.; Soleymanabadi, H. Theoretical study on the Al-doped ZnO nanoclusters for CO chemical sensors. *J. Phys. Chem. C*. **2015**, 119 (11), 6398.

(58) Zhu, H.; Zhao, C.; Cai, Q.; Fu, X.; Sheykhahmad, F. R. Adsorption behavior of 5-aminosalicylic acid drug on the B12N12, AlB11N12 and GaB11N12 nanoclusters: A comparative DFT study. *Inorg. Chem. Commun.* **2020**, *114*, 107808.

(59) Johnson, E. R.; Keinan, S.; Mori-Sánchez, P.; Contreras-García, J.; Cohen, A. J.; Yang, W. Revealing noncovalent interactions. *J. Am. Chem. Soc.* **2010**, *132* (18), 6498–6506.

View Article Online
DOI: 10.1039/D5NA01168J

Data Availability Statement

The datasets generated and analyzed during the current study are available from the corresponding author upon reasonable request.